

Review paper

Thermal shock resistance of magnesia–chrome refractories—experimental and critical evaluation

J. Wojsa*, J. Podwórny, R. Suwak

Institute of Ceramics and Building Materials, Refractory Materials Division, ul. Toszecka 99, 44-100 Gliwice, Poland

Received 22 February 2012; received in revised form 30 May 2012; accepted 31 May 2012

Available online 13 June 2012

Abstract

Eleven commercially available magnesia–chrome refractories have been tested. Their basic properties have been determined along with bending strengths at 20, 950 and 1400 °C, linear thermal expansion coefficients at 950 °C and 1400 °C, Young's modulus by the static method and the work of fracture at 950 °C. Young's modulus was determined within the temperature range 20–1000 °C, in the process of heating and cooling. The values of thermal shock resistance R_{st} and R_4 were calculated and correlated to thermal shock resistance (TSR). It has been demonstrated that the R_{st} criterion is a useful tool to forecast TSR, no matter whether the value of the E modulus is determined by the static or dynamic method. The values of Young's modulus obtained by various methods at 20 °C and 950 °C have been compared. It has been proven that Young's modulus dependence on temperature is a specific feature of a given material.

© 2012 Published by Elsevier Ltd and Techna Group S.r.l.

Keywords: C. Thermal shock resistance; D. Spinels; E. Refractories; Magnesite–chrome materials

Contents

1. Introduction	1
2. Experimental procedure	3
3. Evaluation of measurement uncertainty	4
4. Results and discussion	4
5. Conclusions	9
Acknowledgement	12
References	12

1. Introduction

Magnesia–chrome materials used to be a dominant variety of basic refractories. The technological development of magnesia–carbon materials and their wide applicability in thermal equipment used in iron metallurgy, similarly to a kind of material revolution in the field of magnesia–spinel and other varieties of chrome-free

materials applied in refractory linings for rotary kilns in the cement industry, have considerably reduced the application range of Cr_2O_3 -containing materials.

However, in many secondary metallurgy processes in ferrous metallurgy as well as in the metallurgy of copper and lead they are still used on a large scale.

Among specialists prevails the opinion that the causes of refractories' wear in ca 70% result from chemical corrosion, and in ca 20% from thermal shocks, while the remaining 10% causes are due to erosion, deformation of furnace jackets and other mechanical factors. For this

*Corresponding author. Tel.: +48322701859; fax: 48322701934.

E-mail addresses: j.wojsa@icimb.pl, sawoj@imo.gliwice.pl (J. Wojsa).

reason, thermal shock resistance and, in particular, the methods of its determination and forecasting remain the subject of investigations carried out by both researchers and practitioners in fields such as manufacturing technologies, refractories design and the use of thermal equipment.

Classic refractories are coarse-grained, porous and, most frequently, multi-phase materials. Their specificity lies in the fact that the very occurrence of internal defects, including cracks, does not determine the loss of their value in use, whereas the propagation of cracks may lead to actual damage of the material under thermal shock conditions. This is the reason why the attention of specialists is focused on criteria related to crack propagation.

In the works [1,2] providing a theoretical basis for a description of crack initiation and propagation, Hasselman presented two criteria characterising the resistance of a material to thermal shocks:

$$R_4 = \frac{EG}{S_t^2(1-\nu)} \quad (1)$$

referred to as thermal shock damage resistance parameter and

$$R_{st} = (G/E\alpha^2)^{1/2} \quad (2)$$

referred to as thermal stress crack stability parameter. Here, E is Young's modulus, G is work of fracture, S_t is tensile strength, ν is the Poisson ratio, and α is the linear thermal expansion coefficient.

In further publications of this author, the R_4 and R_{st} criteria were referred to as "thermal shock resistance parameters". Thus R_4 and R_{st} describe unstable and stable crack propagations, respectively.

Hasselman and Larson have demonstrated that the behaviour of materials under thermal shock conditions depends not only on their properties, but also on the nature of shocks[3]: sudden heating causes a catastrophic development of microcracks, while sudden cooling is accompanied by their stable growth. Investigations were conducted for high-alumina products.

Thermal shock resistance (TSR) is a function of the dimensions and shape of a sample and the nature of thermal shock.

Many theoretical and experimental works have been focused on the forecasting of the behaviour of materials subjected to thermal shocks. The forecasting of TSR is useful for technology specialists who design the composition and the manner of materials manufacture as well as for users, allowing them to select materials from many available varieties. When discussing the influence of microstructure on TSR, Bradt and Harmouth make use of the brittleness number B and characteristic length l_{ch} [4]. These parameters are defined as follows:

$$B = \frac{S_t^2 L}{G_F E} \quad (3)$$

$$l_{ch} = \frac{G_F E}{S_t^2} \quad (4)$$

where S_t is the tensile strength (Pa), L the significant sample dimension (m), E the Young modulus (Pa), and G_F the specific fracture energy (J/m²).

In the opinion of the authors, the brittleness of materials increases as B grows and l_{ch} drops. It is noteworthy that the brittleness number B is in fact the inversed R_4 criterion, as the L sample dimension serves chiefly the purpose of standardisation. The characteristic length l_{ch} is practically identical with the R_4 criterion, and differences in literature data might be related to the manner of G_F determination by means of the wedge splitting test (WST) or three-point bending test.

Naturally, TSR of refractories depend on their microstructure, especially on the length and type of developing microcracks: through the matrix, along the matrix–grain interface or in a transgranular manner. These issues are the subject of many studies, the examples of which are publications [4,5].

The aim of this work is quite different. Investigations into 11 varieties of commercially available magnesia–chrome materials manufactured by 5 European producers were conducted, the values of R_4 and R_{st} were determined, and correlation coefficients for the dependence of thermal shock resistance on R_{st} and R_4 were determined. If the resistance criteria resulting from Hasselman's theory are to be employed in TSR forecasts, they should remain useful not only for specially prepared laboratory samples, but also for commercial products, as this is the real measure of their usefulness.

The model phase composition of magnesia–chrome materials under equilibrium conditions is as follows: periclase, one or two silicates, depending on the CaO/SiO₂ ratio, a spinel solid solution having the following formula: (Mg, Fe II) (Al, Fe III, Cr)₂O₄ and pores. In real materials the state of equilibrium is not achieved frequently, especially in the case of spinel phase. In reality a number of local equilibria with different proportions of Cr₂O₃, Fe₂O₃ and Al₂O₃ are observed, which result from the composition and particle size distribution of raw materials used.

This picture is overlapped by a complex mechanism of "order–disorder" phase transitions, which has not been fully explored. Investigations into pure spinels MgAl₂O₄, MgFe₂O₄ and MgCr₂O₄ showed that in MgAl₂O₄ spinel the beginning of inversion, i.e. the change of a normal structure into an inversed one, takes place at 610 °C, in magnesioferrite (MgFe₂O₄) at 500 °C (the inversed structure changes into a normal one), and MgCr₂O₄ spinel is structurally stable within a 25–1100 °C temperature range, displaying however a constant degree of inversion reaching ca 9%. The conclusions have been based on the measurements of a cation–anion distance in octahedral and tetrahedral positions as well as on the oxygen parameter [6]. In solid spinel solutions the picture is even more complex, as the direction and range of structural changes depend on

the solution's chemical composition, and the phase transition is accompanied by a change in the linear coefficient of thermal expansion [7].

In the conditions of alternate cooling and heating cycles these phenomena create a very dynamic system, whose effective description in criterion-referenced terms does not seem possible. Worth mentioning is the fact that structural transitions of spinels occur at temperatures very different from the temperatures of liquid phase formation in good quality magnesia–chrome materials, which usually takes place at a temperature higher than 1300 °C.

In this work the E modulus values determined by the static and dynamic methods have been compared; also the influence of temperature on the E modulus changes in the process of heating and cooling has been examined. Three methods have been used to experimentally verify the TSR criterion-referenced evaluation:

- TSR as a function of R_{st} and R_4 for the E modulus value determined by the static and dynamic methods,
- dependence of bending strength at T_{max} on $\Delta T = T_{max} - 20$ °C (modified Larson and Hasselman's test [3])
- and TSR dependence on E after 3 thermal shocks.

2. Experimental procedure

- chemical composition has been determined according to PN-EN ISO 12677:2005 (XRF),
- open porosity and apparent density according to PN-EN 993-1:1998,
- cold crushing strength according to PN-EN 993-5:2001,
- modulus of rupture according to PN-EN 993-6:2008 and PN-EN 993-7:2001 (950 °C:1450 °C),
- linear coefficient of thermal expansion according to PN-EN 993-19:2006,
- dynamic E modulus by the resonance method according to ASTM C-1259-94 ($150 \times 25 \times 25$ mm³ beam), measured at 20 °C.

Work of fracture: the method of three-point bending of a $25 \times 25 \times 150$ mm³ beam with a notch having a depth of 8 mm and a width of 0.5 mm, loading rate of 20 μ m/min, measuring system deformation correction, equipment-Netzsch HMOR422. Total deformation of the measuring system and the sample is measured by means of an extensometer, next correction being equal to the measuring system deformation, which is experimentally determined versus temperature, is subtracted. The work of fracture G_F has been calculated from the following formula:

$$G_F = \frac{\int F(dx)}{2A},$$

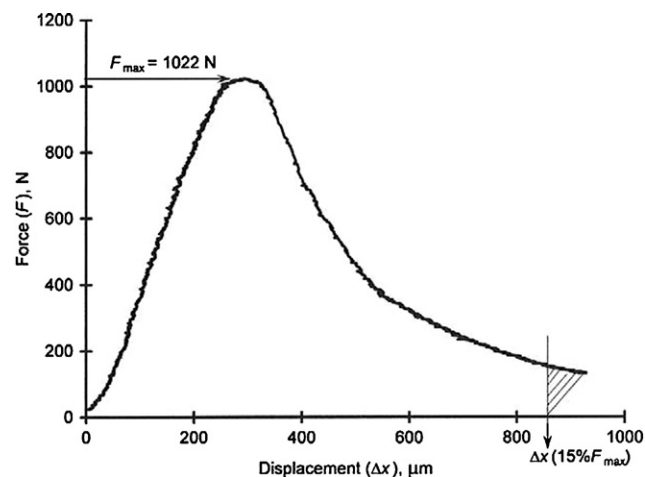


Fig. 1. Illustration of the WOF determination method—force (F) vs. displacement (Δx).

Where F is the force (N), x , the deformation (m) and A is the specimen cross-sectional area (m²).

In order to avoid the influence of compressive stresses in the upper part of the sample, the field under the curve was measured until the value of deformation corresponding to 15% maximal force to the right of the maximum value was obtained. The results of refractories' WOF (work of fracture) measurements have been published since the early 1960s [1,5,8–12]. There are many varieties of WOF determination methods. An example of the force versus deformation dependence is shown in Fig. 1.

- Thermal shock resistance, $\phi = h = 50$ mm cylinders cut out of products, cycles 950 °C/25 min, water/3 min until a 20% loss of specimen volume was obtained.
- Air thermal shocks ($T_{max} = 200$ °C), air pressure 0.1 MPa/5 min, $T_{max} = 400, 600, 700, 800, 900, 1000, 1100$ and 1200 °C and determination of the modulus of rupture at T_{max} after 5 air shocks ($T_{max} - 20$ °C)
- The relationship between the modulus of elasticity and temperature in the process of heating and cooling within a temperature range of 20–1000 °C has been determined. Determinations were carried out at IMCE laboratory (Genk – Belgium) by RFDA (resonant frequency and damping analyser) dynamic method. The dimensions of beams were $25 \times 20 \times 150$ mm³, the heating and cooling rate was 3 °C/min and the samples were soaked at 1000 °C for 30 min. Three samples of each material were taken in order to evaluate the reproducibility of measurements
- The static E modulus at 950 °C has been determined from $F(x)$ graphs, where F is a force, and “ x ” is deformation, which were obtained when determining the work of fracture. On the left branch of the $F(x)$ curve a straight line segment, the linearity of which was verified by calculating the square of r coefficient correlation, was determined. The calculations took into account segments of straight lines for which r^2 was higher or equal to 0.95. When determining the height of

specimens, allowances were made for the depth of notches for each specimen with an accuracy of 0.05 mm. The E modulus was determined from the following dependence:

$$E = \frac{l^3 \Delta F}{4bh^3 \Delta x} \quad (5)$$

Where l is the distance between supports (m), b the specimen width (m), h the specimen height (m), F the force (N) and x the deflection (m).

- Thermal shock resistance depending on the E_3/E_0 ratio, where E_3 is the value of Young's modulus after three thermal shocks (950 °C—water), and E_0 is the value of this modulus before shocks; the modulus was determined by the resonance method at ambient temperature.

All the presented results are average values of minimum three measurements.

3. Evaluation of measurement uncertainty

In the evaluation of measurement uncertainty it has been assumed that there are 2 sources of deviations from the real value:

- 1) an error in the calculations of the E modulus, strength and the work of fracture, resulting from the accuracy of measurement of linear dimensions, force and frequency, estimated by the total differential method (U_1)
- 2) an error resulting from the dispersion of properties within a batch of examined materials, estimated by the standard deviation to average value ratio (U_2).

Relative total uncertainty U is determined from the formula $U = (U_1^2 + U_2^2)^{1/2}$ expressed in % of the average examined value.

The following results of the average value in relation to total uncertainty have been obtained for particular determinations:

- E modulus at 950 °C, static method, E_s (950 °C): 21.3%
- E modulus at 950 °C, measured in the process of heating, resonance method, $E_d(950 \text{ °C})_h$: 8.0%
- E modulus at 950 °C, measured in the process of cooling, resonance method, $E_d(950 \text{ °C})_c$: 4.1%
- work of fracture at 950 °C: 20.1%
- bending strength at 950 °C and 1450 °C: 11.2%
- thermal shock resistance 11.8%
- linear coefficient of thermal expansion within a range of 500–1500 °C 10.5%

In all the cases, the dominant component of uncertainty was the dispersion of properties within a set of specimens (U_2). The component connected with a determination error itself was smaller by minimum one order of magnitude.

4. Results and discussion

Eleven varieties of commercially available magnesia–chrome products containing 19.5 to ca 27 wt% of Cr_2O_3 have been tested. These products were manufactured by 5 well-known European producers and the rationality behind their comparison results from the fact that they are sometimes used as an alternative solution in the same areas of metallurgy, e.g. in thermal equipment linings in the metallurgy of lead, copper and copper alloys.

The chemical composition of the products has been presented in Table 1. The analyses do not include ignition losses as the samples were first fired at 1000 °C.

Table 2 presents basic properties of the examined products as well as their thermal shock resistances, work of fracture measured at 950 °C, bending strength at 20, 950 and 1450 °C and linear thermal expansion coefficient. The intention of the authors is to correlate thermal shock resistance to the values of criteria which are a combination of mechanical and thermal properties. For this reason, the work of fracture was determined at 950 °C as due to order–disorder transitions in spinels and the closing or opening of cracks in a heating or cooling process, the rationality behind measuring the work of fracture at ambient temperature in the case of this group of materials may raise doubts. On the other hand, in good quality magnesia–chrome materials the liquid phase appears at a temperature exceeding 1300 °C, and the selected temperature of 950 °C is sufficiently distant from it.

In the criterial methods of ceramics thermal shock resistance evaluation, the key role is played by two values: the work of fracture and Young's modulus. The remaining values, i.e. thermal expansion coefficient and bending strength (introduced in place of tensile strength, which is difficult to determine) are routinely determined with high accuracy. Poisson's ratio, the value of which is frequently assumed as 0.2 or neglected, raises most controversies because, as shown in the earlier study of the authors [13], due to thermal shocks it may adopt even negative values, which defies intuition. The work of fracture is determined by means of a wedge splitting test (WST) or by three-point bending. The advantage of WST lies in the size of fracture area, which is ca 10 times bigger than that in the case of three-point bending, whereas the asset of the other method is the incomparably greater availability of equipment which allows carrying out determinations. If mechanical stresses are a necessary condition for the occurrence and propagation of a crack, the key value is the modulus of elasticity (–), in particular its dependence on temperature. This dependence can be examined by dynamic (resonance or ultrasonic) or static, i.e. mechanical methods.

Changes to Young's modulus for the selected five materials depending on temperature in the conditions of heating at a maximum temperature of 1000 °C and cooling were made at the laboratory of IMCE (Genk—Belgium) by means of a resonant frequency and damping analyser (RFDA). Changes in the E modulus and damping versus

Table 1

Material designation	Content(wt%)								
	SiO ₂	Al ₂ O ₃	Fe ₂ O ₃	TiO ₂	CaO	MgO	Cr ₂ O ₃	MnO ₂	V ₂ O ₅
1	1.21	6.05	10.25	0.16	0.85	59.23	21.97	0.08	0.09
2	1.17	4.46	7.87	0.13	0.85	63.98	21.28	0.08	0.07
3	1.56	5.07	9.63	0.18	0.77	59.41	23.11	0.08	0.08
4	1.55	6.43	9.44	0.15	0.59	60.48	21.08	0.08	0.09
5	1.30	7.71	10.87	0.18	0.53	55.17	23.93	0.08	0.10
6	0.97	5.91	12.17	0.21	0.87	59.35	20.23	0.07	0.10
7	1.33	4.20	9.23	0.07	1.23	60.97	22.73	0.07	0.03
8	1.02	6.20	12.39	0.22	0.91	57.16	21.77	0.08	0.11
9	1.00	5.93	9.07	0.09	0.65	56.22	26.78	0.07	0.06
10	0.84	6.00	13.32	0.22	1.29	58.27	19.53	–	0.12
11	0.78	6.08	13.58	0.25	1.22	58.26	19.42	–	0.13

Table 2

	Open porosity (%)	Apparent density (g/cm ³)	Compressive strength (MPa)	Gas permeability (nPerm)	TSR, cycles 950 °C/ 25 min, water/3 min	Bending strength (MPa)			Work of fracture (J/m ²)	Linear thermal expansion coefficient (°C ^{−1})	
						22 °C	950 °C	1450 °C		950 °C	1400 °C
1	15.7	3.16	41.8	8.3	8.3	9.8	12.5	2.8	148.5	10.2	11.2
2	13.7	3.21	64.8	2.3	9.3	7.0	11.6	3.7	114.0	9.64	10.7
3	12.3	3.30	53.9	1.9	8.3	16.3	10.0	2.9	122.9	9.68	10.8
4	17.2	3.08	54.0	4.6	10.0	5.1	8.7	3.8	137.6	10.3	11.4
5	18.5	3.08	27.8	9.7	9.6	3.0	5.2	1.7	77.4	9.5	10.7
6	13.7	3.24	37.1	4.3	9.3	4.0	6.2	0.95	156.5	9.9	10.8
7	16.1	3.13	31.7	6.5	13.6	4.0	4.1	0.65	159.1	10.1	10.8
8	13.3	3.27	39.2	4.9	7.6	4.0	7.8	2.8	178.8	9.69	10.7
9	15.4	3.20	45.1	4.3	8.0	4.0	10.1	3.8	47.0	9.3	10.2
10	15.2	3.26	64.3	8.4	14	8.0	8.3	–	147.8	10.2	10.8
11	15.0	3.27	61.7	6.1	12.5	8.2	12.9	4.4	211.4	9.4	10.5

temperature have been shown in Figs. 2–6. A good repeatability of determinations with regard to the shape of curves as well as the modulus and damping values is noteworthy. This is a real “finger print” determination. It should be emphasised that for investigations, materials differing in their thermal shock resistance have been selected (see Table 2).

The modulus value at 950 °C in a heating and cooling process was read off from the $E(T)$ dependence graphs. In the further part of the work this modulus will be referred to as dynamic and determined as $E_d(950\text{ °C})$ with an “h” (heating) or “c” index (cooling).

The E modulus value was also determined by the static notched beam method while determining the work of fracture at 950 °C [$E_s(950\text{ °C})$].

Table 3 presents the results of the E modulus measurement, including a resonance method test carried out at ambient temperature, determined as $E_d(20\text{ °C})$.

The authors were somewhat surprised by the results of investigations into Young's modulus dependence as, in the process of heating, the modulus value for materials 1, 4 and 7

grew, while for materials 10 and 11 it dropped to reach temperatures of ca 600 and ca 700 °C respectively, and then increased to reach 1000 °C. The common feature of all the examined materials is an evident growth of the $E_d(T)$ curve slope, starting with the temperature of ca 600 °C (materials 1 and 4) and ca 700 °C (material 7) as well as ca 750 °C and 800 °C for materials 11 and 10 respectively. This is most probably related to both the spinel component phase transition (we intentionally do not use the term “spinel phase”) and the closing of microcracks. The dwelling of samples at 1000 °C for 30 min, followed by their cooling, causes an evident increase of the modulus with considerable maximum values in the case of samples 1 and 4, and its relatively slow drop for the remaining samples. Cooling brings about a high increase in damping, the intensity of which is specific to each of the examined materials.

Correlating the modulus and damping changes with the microstructure is not the subject of this work, but the obtained dependences open a new area of research, which seems even more interesting due to the fact that the modulus measured by the dynamic method, E_d , is considerably higher

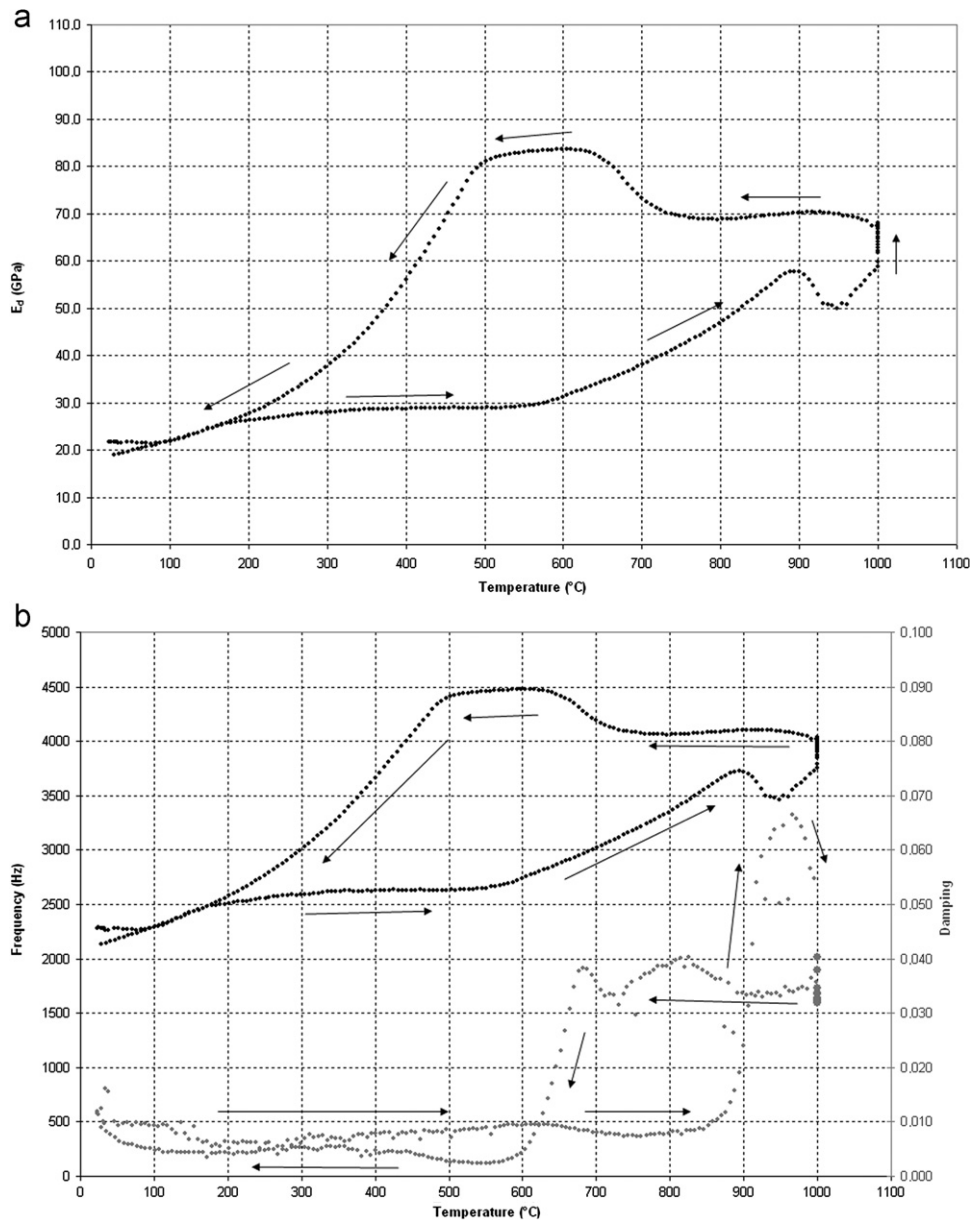


Fig. 2. Dependence of the elasticity modulus (a) as well as frequency and damping (b) on temperature—material 1.

than that determined by the static method, E_s , and differs significantly from the value determined by the resonance method at 20 °C, $E_d(20\text{ °C})$.

The data contained in Table 3 are a good illustration of errors that may be committed when engineering calculations are based on modulus values determined by the dynamic method at ambient temperature.

The determined values of thermal shock resistance (TSR), work of fracture and thermal expansion coefficients (Table 2) as well as Young's modulus (Table 3) allowed investigating the correlation among TSR, R_{st} and R_4 . An independent variable is the criterion (R_{st} and R_4), as forecasting consists in evaluating the behaviour of a material subjected to high temperature gradients on the basis of previously determined material properties.

R_{st} and R_4 were calculated for Young's modulus values given in Table 3, i.e. $E_s(950\text{ °C})$, $E_d(950\text{ °C})_h$ and $E_d(950\text{ °C})_c$. A linear functional dependence $TSR=f(R_{st})$ was determined and correlation coefficients were calculated. To complete the data on bending strength at 950 °C (Table 3), the value of R_4 criterion was calculated (the value $v=0$ was adopted) and correlation coefficients were also determined for the linear dependence $TSR=f(R_4)$. The results of calculations have been presented in Table 4 and in Fig. 7. These results show that TSR grows linearly with R_{st} .

The classical theory of Hasselman [2] suggests the following physical meaning of this dependence: R_{st} is a coefficient of proportionality between the critical temperature difference ΔT_c causing the unstable propagation of a

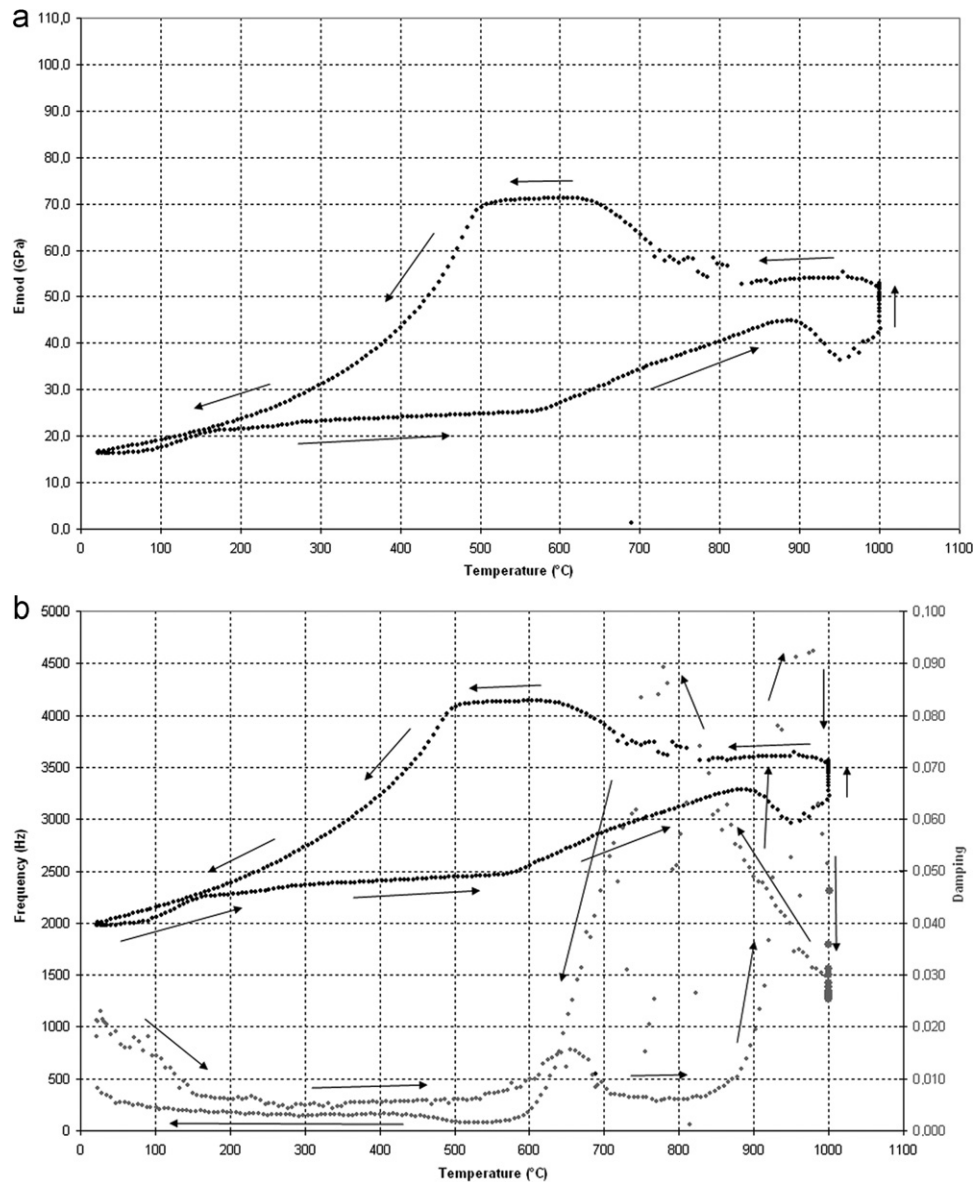


Fig. 3. Dependence of the elasticity modulus (a) as well as frequency and damping (b) on temperature—material 4.

crack and the complex function of Poisson's ratio, the crack length and the density of cracks. This means that growing R_{st} values should be accompanied by an increase in the critical temperature difference, provided that the remaining parameters are constant.

From the value of correlation coefficients for the $TSR(R_{st})$ and $TSR(R_4)$ dependences it may be concluded that if this method of inducing thermal shocks is applied, the resistance of magnesia–chrome materials is dependent on the mechanism of the stable development of crack length (R_{st}) to a far greater degree than on the catastrophic mechanism (R_4).

The significance of $TSR(R_{st})$ correlation coefficients given in Table 4 was evaluated by means of Student's test t [14]. It has been demonstrated that the level of significance for coefficients 0.843, 0.968 and 0.963 is $\alpha=0.01$, and for the correlation coefficient $r=0.934$, $\alpha=0.05$. The

significance of $TSR(R_4)$ correlation was not verified due to the low values of correlation coefficients.

Taking into consideration the fact that the object of investigations are commercial materials, the obtained dependences may be deemed satisfactory.

Some light on the character of changes to the work of fracture depending on temperature was cast by determinations carried out for materials Nos. 1, 5 and 11 at 450, 700, 950 and 1200 °C.

The results of measurements have been given in Table 5. The values of the work of fracture at 950 °C for materials 1 and 11 differ from the values presented in Table 2, which results from the unavoidable dispersion of commercial products properties. These differences are not big, though. It is worth mentioning that the work of fracture at 950 °C is notably higher compared to the value at 700 °C. These temperatures approximately correspond to the beginning

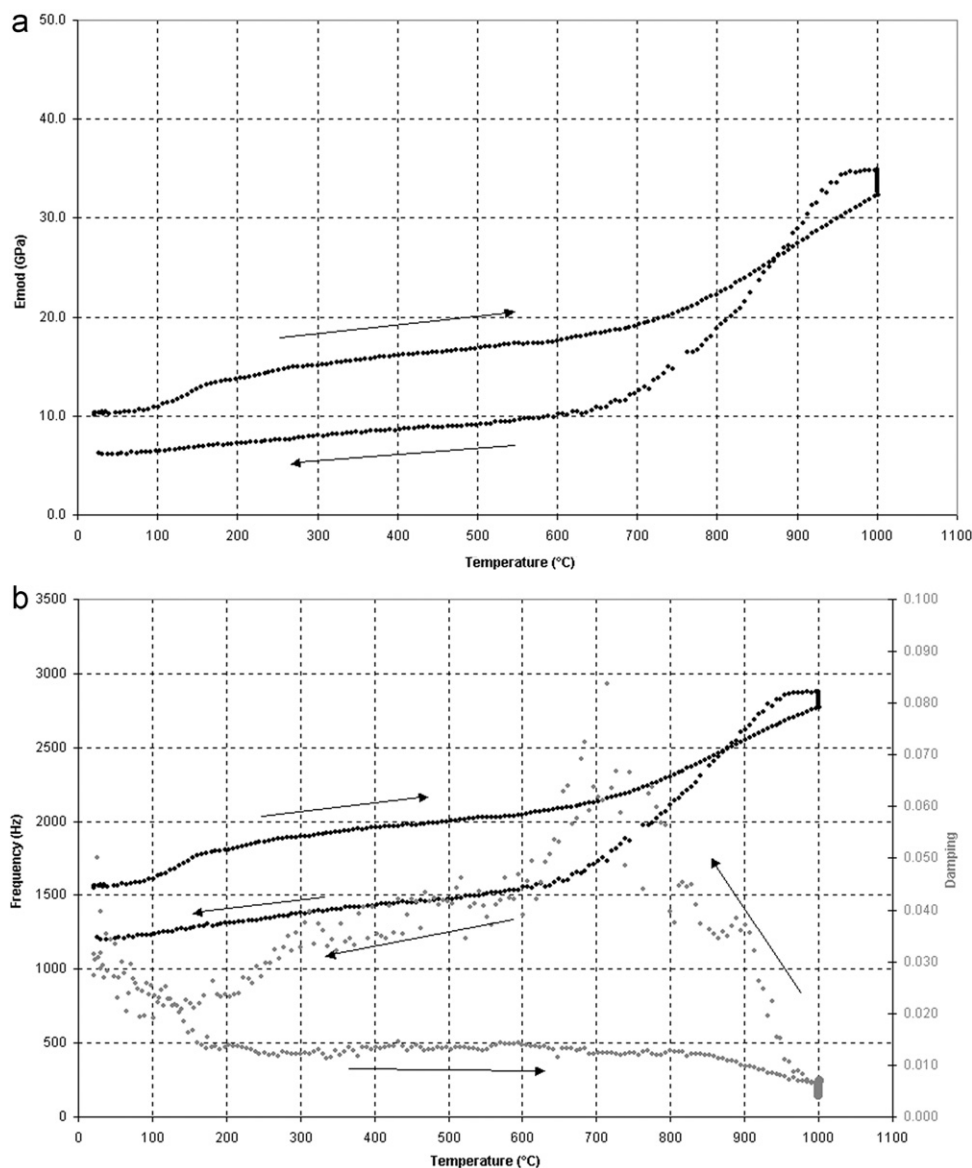


Fig. 4. Dependence of the elasticity modulus (a) as well as frequency and damping (b) on temperature—material 7.

and the end of the reversible order–disorder transition in spinels.

A further high increase in the value of the work of fracture at 1200 °C most probably results from the growing share of plastic deformation of the examined materials, with no participation of the liquid phase. Another method of thermal shock resistance evaluation consists in measuring the changes in mechanical strength, e.g. bending strength at ambient temperature, depending on thermal shock intensity, ΔT [3].

The authors of this work have modified the known procedure in the following way: samples in the shape of beams were subjected to 5 air thermal shocks with temperature difference $\Delta T = T_{max} - 20$ °C, within the range T_{max} (400–1200 °C); after 5 shocks the value of bending strength at T_{max} was determined. The results of investigations have been shown in Fig. 8.

Starting with a temperature of 900 °C, the values of bending strength for the tested materials correspond to their thermal shock resistance, and given the uncertainty of bending strength measurements, significant differences begin to be observed at a temperature of 1000 °C. The applied research procedure fulfils the requirement of bearing resemblance to real conditions of a thermal shock and may provide a basis for developing a standard determination of TSR. The issue needs to be further investigated.

The third way of evaluating TSR of magnesia–chrome materials involved measuring Young's modulus by the resonance method before (E_0) and after 3 thermal shocks 950 °C—water (E_3). After each shock the $150 \times 25 \times 25$ mm³ beams were dried at 120 °C and annealed at 500 °C in order to remove any effects of hydration. The correlation between TSR expressed by the number of cycles (Table 2) and the E_3/E_0 ratio expressed in %

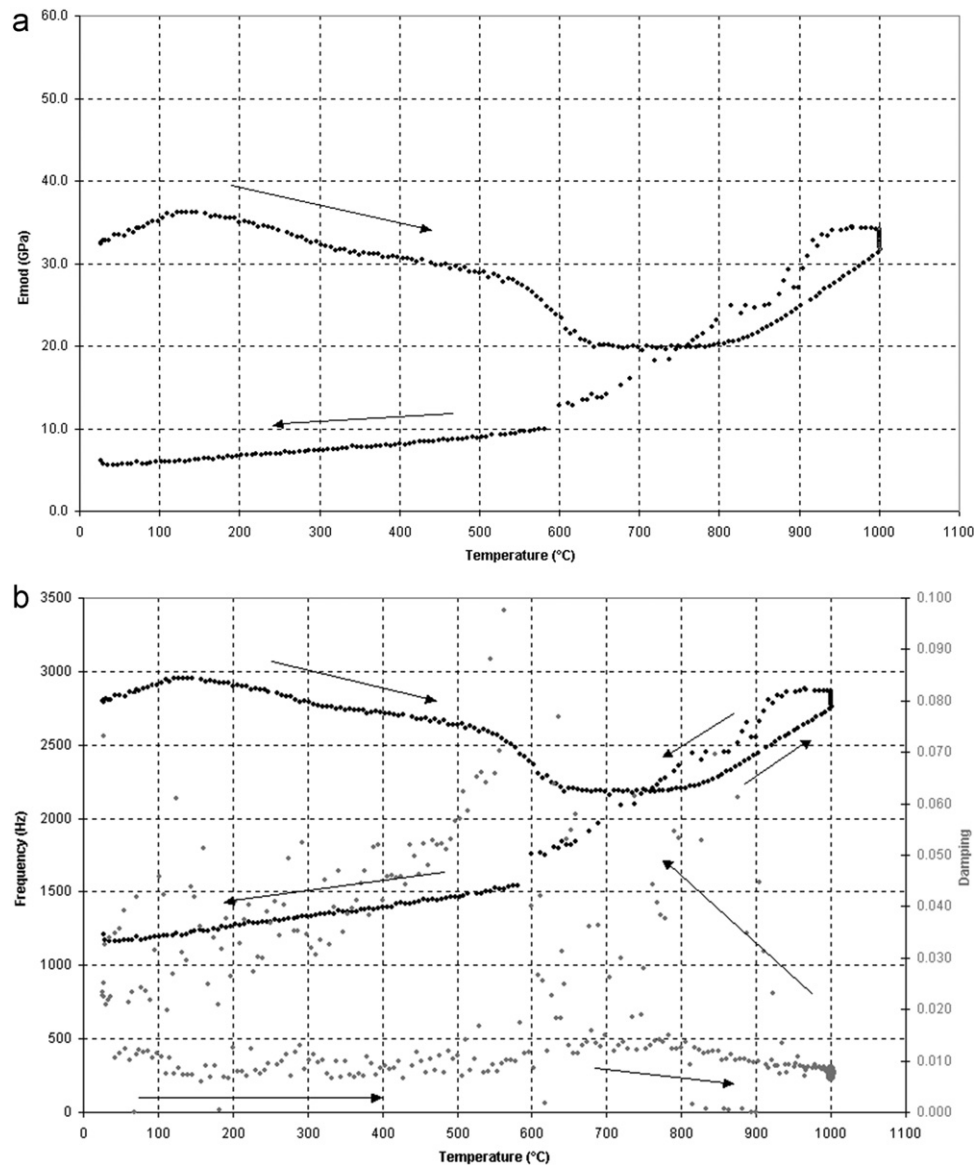


Fig. 5. Dependence of the elasticity modulus (a) as well as frequency and damping (b) on temperature—material 10.

was verified. The revealed picture of dependences was a set of chaotically scattered points and the calculated correlation coefficient (-0.162) excludes the existence of any sensible relationship.

5. Conclusions

1. It has been proven that magnesia–chrome materials are characterised by a considerably varied dependence of Young's modulus on temperature within a 20–1000 °C range. For three out of five tested materials, Young's modulus increased with heating up to 600–700 °C, while for the remaining two materials it dropped. The common feature of the materials is that the modulus value increase at temperatures exceeding 750–800 °C. The dependence of Young's modulus on temperature is a specific feature of a

given material, which cannot be forecast on the basis of primary, classical properties of materials.

2. Dwelling at 1000 °C, followed by cooling at a rate of 3 °C/min, causes modulus increase. The degree of this growth and the rate of the modulus value drop in the process of the material's further cooling are also specific features of a material, most probably related to the state of local equilibria within the spinel component.
3. Changes in the modulus and damping may result from two overlapping processes: a reversible “order–disorder” phase transition and the closing or opening of cracks formed due to local differences in thermal expansion as one of the effects of these changes. Given the complexity of the phenomena and their dependence on temperature, the forecasting of materials TSR on the basis of their characteristics obtained at ambient temperature does not seem to be justified.

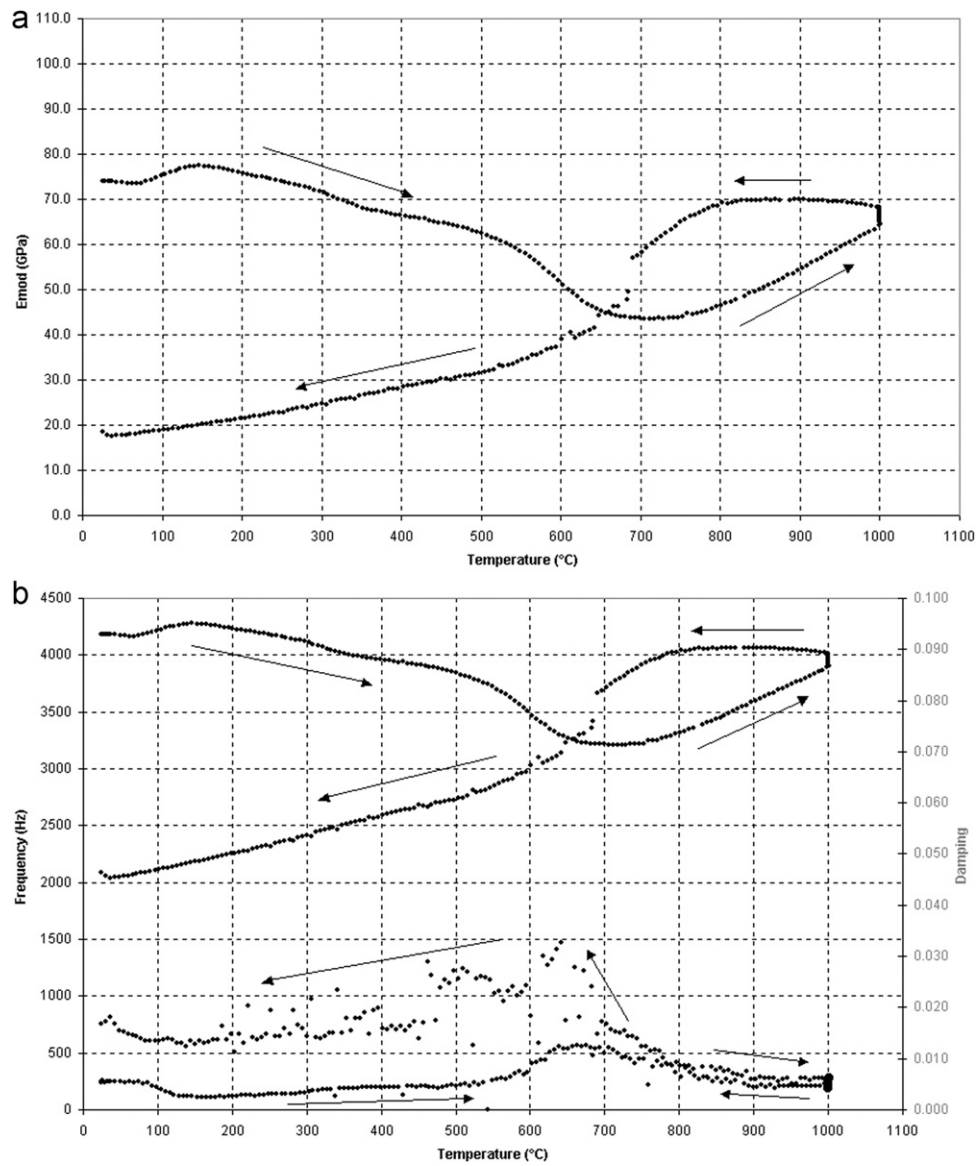


Fig. 6. Dependence of the elasticity modulus (a) as well as frequency and damping (b) on temperature—material 11.

Table 3

Material designation	$E_d(20^\circ\text{C})$	$E_s(950^\circ\text{C})$	$E_d(950^\circ\text{C})_h$	$E_d(950^\circ\text{C})_c$
1	39.1	30.4	53.1	72.0
2	28.0	56.2	—	—
3	54.3	44.6	—	—
4	16.7	15.6	35.2	52.5
5	10.1	14.6	—	—
6	17.2	13.7	—	—
7	7.5	12.3	28.0	31.2
8	13.3	32.9	—	—
9	23.8	45.1	—	—
10	34.2	6.7	28.0	34.0
11	47.1	18.6	55.1	64.7

4. Determination of the work of fracture at 950 °C, Young's modulus by the resonance (dynamic) and static methods, thermal expansion coefficient and bending

strength enabled calculating the values of resistance criteria R_{st} and R_4 for 11 materials. It has been found that there is an acceptable correlation between TSR and

Table 4

Designations of tested materials	Young's modulus, manner of determination	TSR = $f(R_{st})$ dependence		TSR = $f(R_d)$ dependence
		Equation	Correlation coefficient r	Correlation coefficient r
1–11	$E_s(950\text{ }^\circ\text{C})$	TSR = 0.5814 $R_{st} + 5.1753$	0.843	0.014
1, 4, 7, 10, 11	$E_d(950\text{ }^\circ\text{C})_h$	TSR = 2.6362 $R_{st} - 5.4185$	0.968	0.477
1, 4, 7, 10, 11	$E_d(950\text{ }^\circ\text{C})_c$	TSR = 2.1906 $R_{st} - 1.0419$	0.963	0.434
1, 4, 7, 10, 11	$E_s(950\text{ }^\circ\text{C})$	TSR = 0.7981 $R_{st} + 3.2008$	0.934	0.319

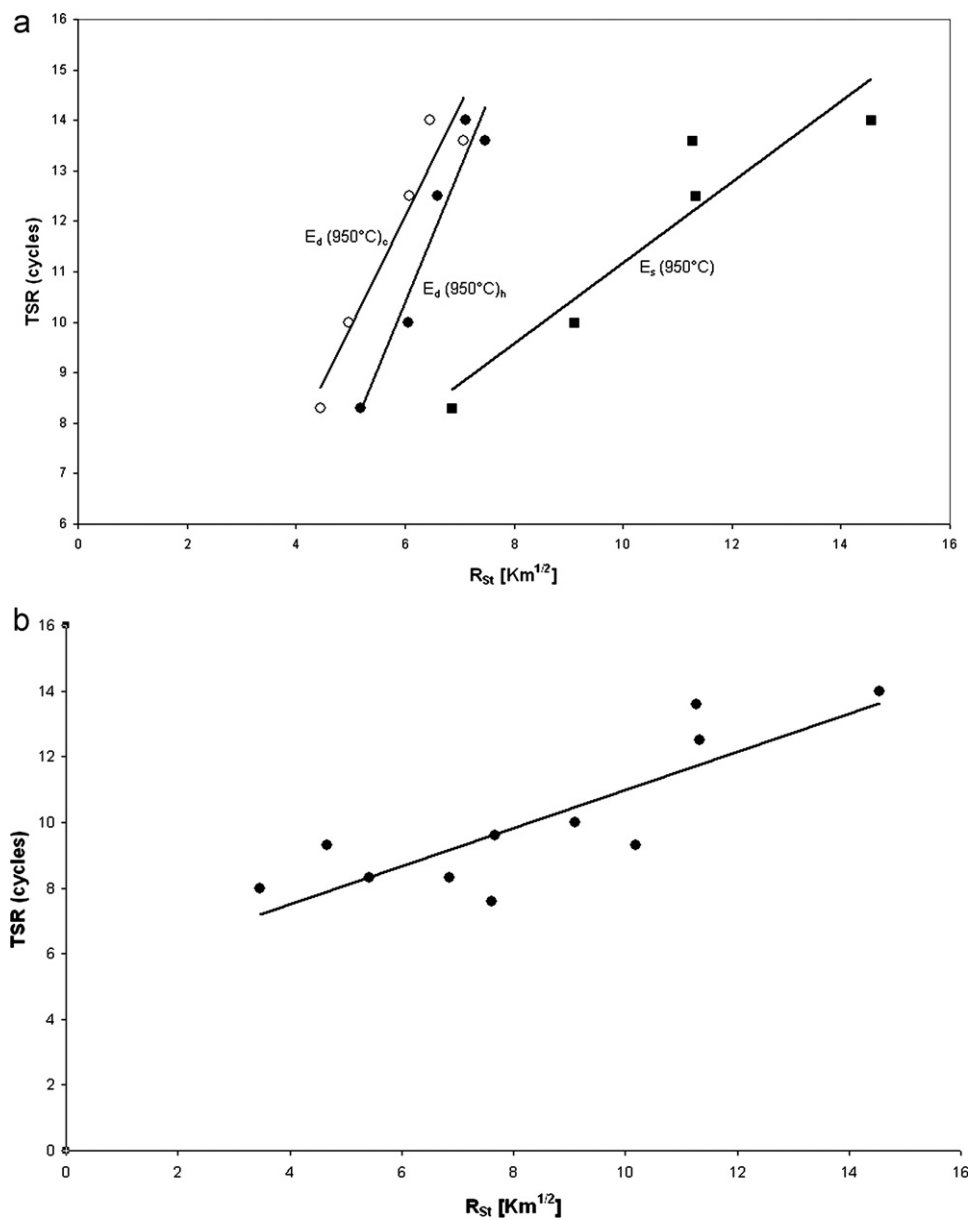


Fig. 7. (a) Dependence of thermal shock resistance (TSR) on the value of the R_{st} criterion calculated for Young's modulus determined at 950 °C by the static and dynamic methods (materials 1, 4, 7, 10, 11); (b) TSR as a function of R_{st} for materials 1–11; Young's modulus determined by the static method at 950 °C. Modulus determination as shown in Tables 3 and 4.

Table 5
Work of fracture (J/m^2) at different temperatures.

Material designation	Temperature T (°C)			
	450	700	950	1200
1	66.2	84.1	143.3	204.2
5	45.1	59.0	77.9	193.6
11	112.9	100.5	198.1	391.3

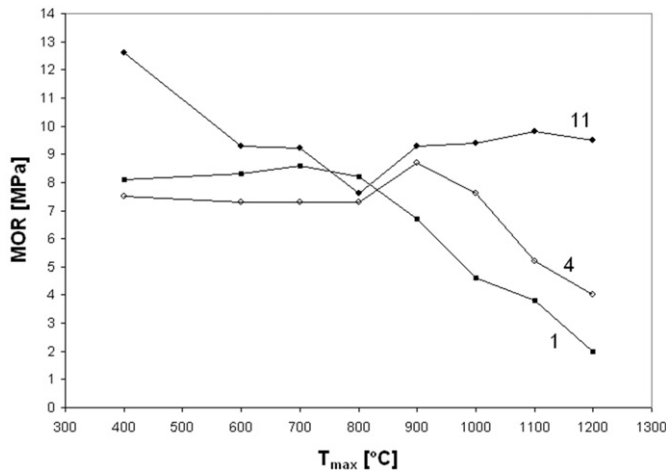


Fig. 8. Bending strength of materials Nos. 1, 4 and 11 at T_{\max} (°C) after 5 thermal shocks (T_{\max} = ambient temperature).

R_{st} , as opposed to the criterion R_4 . From the point of view of this correlation significance, it is possible to use both the static and dynamic moduli determined by the resonance method.

- Apart from the cognitive value, the obtained results also have a practical meaning. The dependence of Young's modulus on temperature given in the form of an equation can be applied in engineering calculations concerning refractory linings, and the compliance of the R_{st} criterion with TSR may be used to select refractories for particular application conditions. Certainly, the said compliance refers solely to the method of TSR determination adopted in this work.
- The dependence of the work of fracture and Young's modulus on microstructure, in particular a description of local equilibria in the spinel component and their influence on TSR, should be the subject of further investigations. Also the reasons for such big differences in the $E(T)$ dependence in the process of heating and cooling as well as the accompanying changes in damping need to be further explained.

Acknowledgement

The presented investigations were conducted within the framework of Ini Tech Project no. ZPB 68/65708/IT2/10 financed by the National Research and Development Centre in Warsaw.

References

- [1] D.P.H. Hasselman, Elastic energy at fracture and surface energy as design criteria for thermal shock, *Journal of the American Ceramic Society* 46 (11) (1963) 535–540.
- [2] D.P.H. Hasselman, Unified theory of thermal shock fracture initiation and propagation in brittle ceramics, *Journal of the American Ceramic Society* 52 (11) (1969) 600–604.
- [3] D.R. Larson, D.P.H. Hasselman, Comparative spalling behaviour of high-alumina refractories subjected to sudden heating or cooling, *Transactions and Journal of the British Ceramic Society* 74 (2) (1975) 59–65.
- [4] R.C. Bradt, H. Harmuth, The fracture resistance of refractories, *Refractories Worldforum* 3 (4) (2011) 129–135.
- [5] J-Lin Cheng Chang-Cheng Chou, Kuan-Jye Chen, Yung-Chao Ko, Fracture energy and thermal stress resistance parameter of high-alumina brick, *American Ceramic Society Bulletin* 65 (7) (1986) 1042–1046.
- [6] J. Podwórny, J. Wojsa, J. Pawluk, J. Piotrowski, Study on increased chemical reactivity of MgAl_2O_4 , MgCr_2O_4 and MgFe_2O_4 spinels at elevated temperature, in: *Proceedings of the Unified Int. Technical Conference on Refractories, UNITECR'07, Dresden, 2007*, pp. 286–289.
- [7] F. Martignago, A. Dal Negro, S. Carbonin, How Cr^{3+} and Fe^{3+} affect Mg–Al order–disorder transformations at high temperature in natural spinels, *Physics and Chemistry of Minerals* 30 (2003) 401–408.
- [8] J. Nakyama, M. Ishizuka, Experimental evidence for thermal shock damage resistance, *American Ceramic Society Bulletin* 45 (7) (1966) 666–669.
- [9] J.A. Rodrigues, V.C. Pandolfelli, M. Rigaud, Elevated temperature thermal shock parameters for refractories, *Interceram* 51 (5) (2002) 322–326.
- [10] J. Wojsa, K. Czechowska, A. Wrona, Prediction of thermal shock resistance of refractory castables, in: *Proceedings of the Stahl u. Eisen Sp. 47th Int Colloquium on Refractories, Aachen (2004)* 35–37.
- [11] B. Alapin, J. Potschke, Investigations of the high-temperature properties of some industrial refractories with the wedge-splitting method, in: *Proceedings of the Stahl u. Eisen Sp. 48th Int Colloquium on Refractories, Aachen, 2005*, pp. 183–189.
- [12] H. Harmuth, K. Rieder, M. Krobath, E. Tschegg, Investigations of the nonlinear fracture behaviour of ordinary ceramic refractory materials, *Materials Science and Engineering A214* (1996) 53–61.
- [13] J. Podwórny, J. Wojsa, T. Wala, Variation of Poisson's ratio of refractory materials with thermal shocks, *Ceramics International* 37 (2011) 2221–2227.
- [14] J. Czermiński, A. Iwasiewicz, Z. Paszek, A. Sikorski, in: *Metody statystyczne w doświadczeniach chemicznych Statistical Methods in Chemical Experiments*, PWN Warszawa, 1970 (in Polish).